

STATISTICAL DYNAMICS OF CONSERVED DENSITIES FOR THE HARD-SPHERE LORENTZ GAS

Joseph W. HAUS

F.B. Physik, GHS Essen, 4300 Essen 1, West-Germany

and

M. LÜCKE

Institut für Festkörperforschung, der Kernforschungsanlage Jülich, 5170 Jülich, West-Germany*
and Institute for Theoretical Physics, University of California, Santa Barbara CA 93106, USA

Received 1 April 1981

The statistical dynamics of a particle scattered by randomly positioned stationary hard spheres are investigated. We examine the somewhat unusual long-wavelength, low-frequency fluctuation spectra resulting from the existence of an infinite set of mutually coupled conserved densities of which the number density and energy density are two members. The analytically soluble infinite-mode correlation functions are compared with the corresponding functions obtained by truncating the set of slow modes at successively increasing orders. Furthermore, we evaluate the long-wavelength number density autocorrelation function for a fixed speed, v_0 , in terms of a frequency-dependent diffusivity $D(\omega; v_0)$ and obtain the fluctuation spectra of all conserved densities by an additional velocity average with the appropriate canonical weights. The effect of the frequency-dependent diffusivity $D(\omega; v_0)$ on the density fluctuation spectra at frequencies small compared to the mean collision frequency is elucidated.

1. Introduction

The dynamics of a classical particle $(\mathbf{r}_0(t), \mathbf{v}_0(t))$ moving in the potential

$$U_0(\mathbf{r}) = \sum_{i=1}^{N_s} u_0(|\mathbf{r} - \mathbf{r}_i|), \quad (1.1)$$

of N_s scatterers fixed at (random) positions $\{\mathbf{r}_i\}$ has received increasing attention recently^{1,2}.

Such a system has two dynamically relevant constants of the motion: particle number $N_0 = 1$ and the particle's energy

$$H_0 = \frac{mv_0^2}{2} + U_0(\mathbf{r}_0). \quad (1.2)$$

Statistical properties of these Lorentz systems have been investigated using microcanonical ensembles within which H_0 was restricted to be the same for every realization of initial conditions $(\mathbf{r}_0, \mathbf{v}_0)$ and scatterer coordinates $\{\mathbf{r}_i\}$.

*Permanent address.

Under these circumstances number density fluctuations

$$\rho(\mathbf{k}, t) = e^{-i\mathbf{k} \cdot \mathbf{r}_0(t)}, \quad (1.3)$$

constitute the only slow mode for long wavelengths. In contrast to dynamical many-body systems here the microcanonical ensemble implies number density and energy density fluctuations

$$\epsilon(\mathbf{k}, t) = H_0 e^{i\mathbf{k} \cdot \mathbf{r}_0(t)}, \quad (1.4)$$

to be statistically and dynamically equivalent.

On the other hand, in a canonical ensemble H_0 is a fluctuating quantity; then the statistical dynamics of ρ and ϵ fluctuations are different although their time evolution for a particular realization of scatterers is the same. Since the currents of (1.3) and (1.4) are not conserved one would conclude that long-wavelength fluctuations of ρ and ϵ in eqs. (1.3) and (1.4) relax diffusively for long times and that their spectra are superpositions of two Lorentzians. However, the situation is more subtle: any function of the form $f(H_0) e^{i\mathbf{k} \cdot \mathbf{r}_0}$ is a density of a conserved quantity, and there is no a priori reason in the Lorentz gas to neglect such modes in comparison with the modes in eq. (1.3), (1.4).

We determine the effect of this infinite set of conserved densities upon the low k , ω fluctuation dynamics of the system. This goal is accomplished along two avenues of approach: in section 2 we introduce the orthogonal polynomials $\{f_n(H_0)\}$ representing any function $f(H_0)$. We evaluate the fluctuation spectra of the conserved densities $u_n(\mathbf{k}) = f_n(H_0) e^{-i\mathbf{k} \cdot \mathbf{r}_0}$ for small k , ω and determine the effect of successively enlarging the above set $n = 1, 2, \dots, N$ of slow modes which are explicitly taken into account by comparing with the analytically solvable result for $N \rightarrow \infty$. In section 3 we first evaluate the low k , ω number density fluctuation spectrum in a microcanonical ensemble for a fixed energy of the particle and then perform a canonical ensemble average of the spectra with the appropriate weightings.

In order to obtain explicit, quantitative results for both approaches we will limit ourselves in this article to a hard-sphere interaction potential

$$u_0(|\mathbf{r}_0 - \mathbf{r}_i|) = \begin{cases} \infty & \text{for } |\mathbf{r}_0 - \mathbf{r}_i| \leq \sigma \\ 0 & \text{otherwise} \end{cases} \quad (1.5)$$

between particle 0 and scatterer i . The simplifying features of such a Lorentz system are: (i) The energy of the moving particle is purely kinetic so that we will henceforth identify the energy as:

$$H_0 = mv_0^2/2. \quad (1.6)$$

Thus, the particle's speed, $v_0 = |\mathbf{v}_0(t)|$, is a constant of the motion. (ii) H_0 (1.6)

is a genuine one-particle quantity which is independent of $\{r_i\}$. Both properties are physically somewhat pathological and do not hold for realistic interaction potentials. For soft potentials not only are changes in the kinetic and potential energy of a particle along its trajectory through the scatterer configuration to be expected; but, what is more important, the energy is statistically a many-particle quantity due to the scatterer positions entering (1.1).

2. Fluctuation spectra of the conserved densities

In this section we evaluate the long-wavelength, low-frequency fluctuation spectra of the conserved densities for a hard-sphere Lorentz gas employing canonical ensemble averages.

2.1. Conserved densities

Consider the set of conserved densities

$$a_n(\mathbf{k}, t) = f_n(H_0) e^{-i\mathbf{k} \cdot \mathbf{r}_0(t)}, \tag{2.1}$$

which are orthonormalized

$$\langle a_n(\mathbf{k}) | a_m(\mathbf{k}) \rangle = \langle a_n^*(\mathbf{k}) a_m(\mathbf{k}) \rangle = \langle f_n(H_0) f_m(H_0) \rangle = \delta_{nm}, \tag{2.2}$$

with respect to the scalar product given in terms of equal time correlation functions. Averages are defined by

$$\langle A \rangle = \frac{\int d\mathbf{v}_0 d\mathbf{r}_0 d\{r_i\} A e^{-\beta(mv_0^2/2)} e^{-\beta(U_0+U)}}{\int d\mathbf{v}_0 d\mathbf{r}_0 d\{r_i\} e^{-\beta(mv_0^2/2)} e^{-\beta(U_0+U)}}, \tag{2.3}$$

where $\beta^{-1} = m\langle v_0^2 \rangle / d$ determines the variance of the velocity distribution in d dimensions and $e^{-\beta U(\{r_i\})}$ is the weight for a particular scatterer configuration $\{r_i\}$ which could be chosen as unity for a system of overlapping scatterers.

As a side remark we mention that our results for the hard-sphere system are insensitive to replacing the annealed average, (2.3), by an average over a quenched scatterer configuration. The distribution of the scatterers does effect the numerical value of the diffusion coefficient, but we are restricting ourselves in this article to a discussion of the correlation functions in the case where the density is sufficiently low so that there exists a nonzero diffusion coefficient.

Let us choose f_1 and f_2 such that

$$a_1(\mathbf{k}, t) = 1 \cdot e^{-i\mathbf{k} \cdot \mathbf{r}_0(t)}, \tag{2.4a}$$

is the number density and that

$$a_2(\mathbf{k}, t) = \frac{(H_0 - \langle H_0 \rangle)}{\sqrt{\langle (H_0 - \langle H_0 \rangle)^2 \rangle}} e^{i\mathbf{k} \cdot \mathbf{r}_0(t)}, \tag{2.4b}$$

is the normalized energy density orthogonal to the particle density mode using the statistical weight defined in eq. (2.3). Let the higher modes $a_n(\mathbf{k}, t)$ be generated by successively orthogonalizing H_0^{n-1} , then it is a straightforward calculation to determine that:

$$f_{n+1}(H_0) = (-1)^n \left(\frac{\Gamma(n+1) \cdot \Gamma(d/2)}{\Gamma(n+d/2)} \right)^{1/2} L_n^{(d/2-1)}(\beta H_0), \tag{2.5}$$

where $L_n^{(d/2-1)}(z)$ is a Laguerre (Sonine) polynomial and $\Gamma(z)$ denotes the Gamma function³). The set of modes so constructed constitute a complete set representing any conserved density of our system.

2.2. Diffusivities

By truncating the set of modes (2.1) at a finite order N , the low k, ω fluctuation spectra

$$S_{nm}^{(N)}(k, \omega) = -\text{Im}[\omega + ik^2 \hat{D}]_{nm}^{-1}, \tag{2.6}$$

of the conserved densities are given in terms of an $N \times N$ diffusivity matrix

$$\begin{aligned} \hat{D}_{nm} &= \lim_{\omega \rightarrow 0} \lim_{k \rightarrow 0} \frac{\omega^2}{k^2} S_{nm}^{(N)}(k, \omega) \\ &= \frac{1}{d} \int_0^\infty dt \langle \mathbf{v}_0(t) \cdot \mathbf{v}_0 f_n(H_0) f_m(H_0) \rangle, \end{aligned} \tag{2.7}$$

which by virtue of the spectral properties of $S_{nm}^{(N)}(k, \omega)$ is positive semidefinite. In the above Kubo relations we used the equation of motion for the densities

$$\partial_t a_n(\mathbf{k}, t) = -i\mathbf{k} \cdot \mathbf{v}_0(t) a_n(\mathbf{k}, t). \tag{2.8}$$

All elements of the diffusivity matrix can be related to the self-diffusion constant

$$D = \hat{D}_{11} = \left\langle \frac{v_0^2}{\nu} \right\rangle \int_0^\infty d\tau \psi(\tau), \tag{2.9}$$

since $\mathbf{v}_0(t) \cdot \mathbf{v}_0 / v_0^2$ averaged over an ensemble of positions $\mathbf{r}_0, \{\mathbf{r}_i\}$

$$\frac{1}{d} \left\langle \frac{\mathbf{v}_0(t) \cdot \mathbf{v}_0}{v_0^2} \right\rangle_{\mathbf{r}_0, \{\mathbf{r}_i\}} = \psi(t\nu), \tag{2.10}$$

depends on time t and speed v_0 only via the distance, $v_0 t$, that the particle has travelled in time t . We obtain the result (2.9) by scaling the time with the frequency,

$$\nu \sim v_0 n_s \sigma^{d-1}, \tag{2.11}$$

at which a particle of speed v_0 collides with the hard spheres of density n_s . Inserting (2.9)–(2.11) into eq. (2.7) we find

$$\frac{\hat{D}_{nm}}{D} = \left\langle f_n(H_0) \frac{v_0}{\langle v_0 \rangle} f_m(H_0) \right\rangle = \left(a_n(\mathbf{k}) \left| \frac{v_0}{\langle v_0 \rangle} a_m(\mathbf{k}) \right. \right). \tag{2.12}$$

The last equality is presented for later use. The velocity average (2.12) yields ($m \geq n$)

$$\begin{aligned} \frac{\hat{D}_{nm}}{D} &= (-1)^{n+m} \frac{1}{4\pi} \frac{\Gamma(d/2)}{\Gamma((d+1)/2)} \left[\frac{\Gamma(n) \cdot \Gamma(m)}{\Gamma(n-1+d/2)\Gamma(m-1+d/2)} \right]^{1/2} \\ &\times \sum_{l=0}^{n-1} \frac{\Gamma(l-1/2)\Gamma(l+m-n-1/2)\Gamma(n-l+(d-1)/2)}{\Gamma(l+1)\Gamma(l+m-n+1)\Gamma(n-l)}. \end{aligned} \tag{2.13}$$

In order to write the matrix of fluctuation spectra for the truncated set of conserved densities in the form (2.6) we have tacitly assumed that: (i) all eigenvalues of \hat{D} are nonzero. This is true if the diffusion coefficient in eq. (2.9) is nonzero, i.e. if the scatterer density is sufficiently low. (ii) The generalized diffusivities $\hat{D}_{nm}(k \rightarrow 0, \omega \rightarrow 0)$ are well-behaved functions with unique limits $\hat{D}_{nm}(0, 0) = \hat{D}_{nm}$. This does not hold if there are other conserved densities coupling to the N explicitly considered ones, thus inducing diffusive poles in $D_{nm}(k, \omega)$ ^[18,4]. If their coupling is sufficiently strong to modify the N -mode result appreciably, it is best to incorporate the extra slow modes explicitly in the matrix formulation (2.6) by enlarging the set of basic modes thereby trying to make the enlarged matrix of generalized diffusivities well-behaved. However, the reader should be aware that there are infinitely many conserved densities which are mutually coupled, as evidenced by the finite off-diagonal elements of the diffusivity matrix \hat{D}_{nm} in eq. (2.13). Hence an N -mode truncation, leading here to an N -pole approximation of the fluctuation spectra (2.6), reproduces the proper analytical structure of $S_{nm}^{(N)}(k, \omega)$ only for $N \rightarrow \infty$.

2.3. Fluctuation spectra – N -mode truncation versus $N \rightarrow \infty$

In order to determine the relative importance of the various modes and the quality of an N -mode approximation we have evaluated the density fluctuation spectra as a function of N and compared with the result in the limit

$N \rightarrow \infty$. For an N -mode truncation the low k , ω spectra

$$\begin{aligned}
 S_{nm}^{(N)}(k, \omega) &= -\text{Im} \sum_{s=1}^N \frac{Z_{nm}^{(N)}(y_s)}{\omega + ik^2 D y_s} \\
 &\approx -\text{Im} \int_0^\infty dy \frac{\rho^{(N)}(y) Z_{nm}^{(N)}(y)}{\omega + ik^2 D y},
 \end{aligned}
 \tag{2.14}$$

are described by N diffusive poles as superpositions of N Lorentzians. The residues $Z_{nm}^{(N)}(y_s)$ adding up to δ_{nm}

$$\sum_{s=1}^N Z_{nm}^{(N)}(Y_s) = \delta_{nm} \approx \int_0^\infty dy \rho^{(N)}(y) Z_{nm}^{(N)}(y),
 \tag{2.15}$$

and the N positive eigenvalues $\{y_s\}$ of the reduced diffusivity \hat{D}_{nm}/D (2.13) were determined numerically.

Let us discuss the large N limit first; then the eigenvalues $\{y_s\}$ are uniformly distributed between a lower one, y_{\min} , tending to zero for $N \rightarrow \infty$, and an upper one, y_{\max} , increasing for large N proportional to \sqrt{N} (cf. fig. 1).

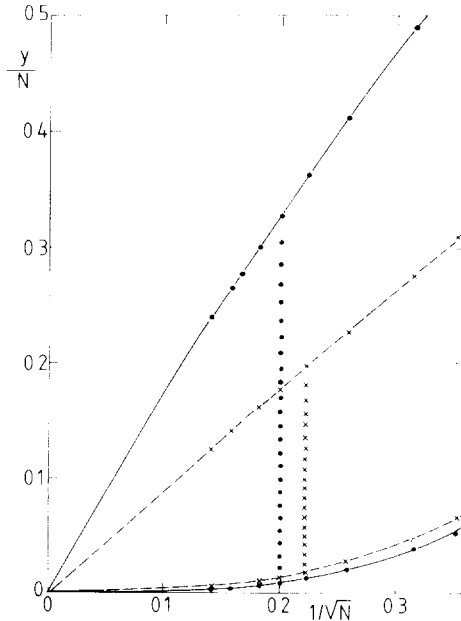


Fig. 1. Eigenvalue extrema of the $N \times N$ diffusivity matrix \hat{D}_{nm}/D , (2.13). Upper and lower dots (crosses) represent y_{\max}/N and y_{\min}/N , respectively, as functions of $1/\sqrt{N}$ for $d = 3$ ($d = 10$). The curves are guides to the eye. For two different values of N the entire range of eigenvalues are inscribed: for $d = 3$ (dots) and for $d = 10$ (crosses).

The density $\rho^{(N)}(y)$ of eigenvalues increases with growing N . Thus, for real ω , we may approximate the sums in (2.14), (2.15) by integrals. The spectral weights $Z_{nm}^{(N)}(y_s)$ are plotted in fig. 2 for $n, m = 1, 2$; $N = 28$ and $d = 3$. They show that the number density fluctuation spectrum $S_{11}(k, \omega)$ is dominated by poles spread around frequencies $-ik^2D$ whereas fluctuations of $\delta H_0 e^{ik \cdot r_0}$ are characterized by at least two different relaxation rates. Furthermore, the damping rates larger than, say, $3k^2D$ do not play a role in the fluctuation dynamics of the first two modes, eq. (2.4).

It is hardly surprising that already the $N = 28$ mode truncation is almost indistinguishable from the $N \rightarrow \infty$ limit. For the latter one obtains from (2.6)

$$\begin{aligned}
 S_{nm}^{(\infty)}(k, \omega) &= -\text{Im}(a_n(k) \left| \frac{1}{\omega + ik^2D(v_0/\langle v_0 \rangle)} a_m(k) \right. \\
 &= -\text{Im} \left\langle \frac{f_n(H_0)f_m(H_0)}{\omega + ik^2D(v_0/\langle v_0 \rangle)} \right\rangle,
 \end{aligned}
 \tag{2.16}$$

by inserting the representation (2.12) of the diffusivity matrix \hat{D}_{nm} together with the completeness of the basis $\{a_n\}$. Hence,

$$S_{nm}^{(\infty)}(k, \omega) = -\text{Im} \int_0^\infty dy \frac{f_n(H_0)f_m(H_0)P(y)}{\omega + ik^2Dy},
 \tag{2.17}$$

where

$$P(y) = y^{d-1} e^{-ay^2} / \int_0^\infty dy y^{d-1} e^{-ay^2},
 \tag{2.18}$$

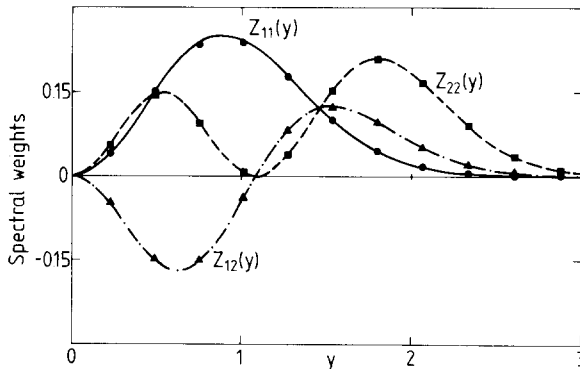


Fig. 2. Spectral weights $Z_{11}^{(N)}(y_s)$ (dots), $Z_{22}^{(N)}(y_s)$ (squares), and $Z_{12}^{(N)}(y_s)$ (triangles) contributing to the correlation spectra $S_{nm}^{(N)}(k, \omega)$ (2.14) for a $N = 28$ mode truncation in $d = 3$ dimensions, as functions of eigenvalues y_s . Curves show $Z_{nm}^{(N)}(y) = f_n(H_0)f_m(H_0)P(y)/\rho^{(N)}$ as function of $y = v_0/\langle v_0 \rangle$. See text for further explanation.

is the probability distribution of the scaled speed $y = v_0/\langle v_0 \rangle$ and

$$a = \beta \langle v_0 \rangle^2 m/2 = [\Gamma((d + 1)/2)/\Gamma(d/2)]^2. \tag{2.19}$$

The convergence of the N mode truncation of $S_{nm}^{(N)}(k, \omega)$ in eq. (2.14) to the infinite mode result $S_{nm}^{(\infty)}(k, \omega)$, eq. (2.17), is attested to by the already mentioned curves in fig. 2, where we plotted $P(y)f_n(H_0)f_m(H_0)/\rho^{(N=28)}(y)$ and inserted the weights $Z_{nm}^{(N=28)}(y_j)$. The value for $\rho^{(N)}(y)$ has been replaced by an average density $\rho^{(N)}$ of eigenvalues. Note that the magnitude of the weights $Z^{(N)} \sim 1/\rho^{(N)}$ decreases with increasing N such that the product $\rho^{(N)}Z^{(N)}$ tends for $N \rightarrow \infty$ to a constant depending on y and d .

Of course, comparison of the spectra $S_{nm}^{(N)}(k, \omega)$, (2.14), directly with $S_{nm}^{(\infty)}(k, \omega)$ is also possible since (2.17) can be explicitly evaluated, e.g. in $d = 3$ dimensions,

$$\begin{aligned} k^2 DS_{11}^{(\infty)}(k, \omega) &= a[1 - x e^x E_1(x)], \\ k^2 DS_{22}^{(\infty)}(k, \omega) &= -\frac{2}{3} a(1 + x) + \frac{2}{3} \left(\frac{3}{2} + x\right)^2 \cdot k^2 DS_{11}^{(\infty)}(k, \omega), \\ k^2 DS_{12}^{(\infty)}(k, \omega) &= \sqrt{\frac{2}{3}} \left[a - \left(\frac{3}{2} + x\right) k^2 DS_{11}^{(\infty)}(k, \omega) \right], \end{aligned} \tag{2.20}$$

where $x = a(\omega/k^2 D)^2$ and E_1 is the exponential integral function³⁾. The above spectra are plotted in fig. 3 together with the deviation (multiplied by 5) of $S_{11}^{(N)}(k, \omega)$ from $S_{11}^{(\infty)}(k, \omega)$ for $N = 2, 5, 15$. The deviation is largest for $\omega = 0$, this frequency being closest to the branch cut in $S_{11}^{(\infty)}(k, \omega)$. The functions

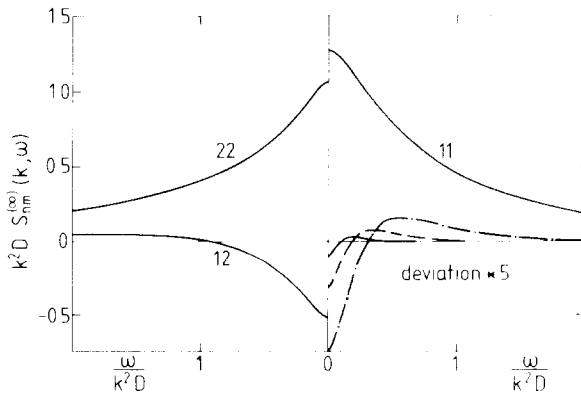


Fig. 3. Reduced density fluctuation spectra $k^2 DS_{nm}^{(\infty)}(k, \omega)$ in $d = 3$ dimensions as functions of $\omega/(k^2 D)$. The deviation $k^2 D[S_{11}^{(N)}(k, \omega) - S_{11}^{(\infty)}(k, \omega)] \times 5$ of the finite mode number density spectrum from the $N = \infty$ result is shown as a representative example for $N = 2, 5, 15$ (dash dotted, dashed, full curve, respectively).

$S_{11}^{(N)}(k, \omega = 0)$ rapidly converge pointwise and monotonously towards zero with increasing N .

2.4. *Remarks*

The most important result of this section is: the density fluctuation spectra of particle number and energy are adequately described at long wavelengths and low frequencies by incorporating only a few of the infinitely many additional conserved densities (2.1) in the matrix description (2.6). The largest deviation of the number density spectrum, for example, is already smaller than 12%^{1f}) if only the coupling to energy fluctuations is explicitly taken care of.

The infinite mode fluctuation spectra $S_{nm}^{(\infty)}(k, \omega)$ are characterized by a branch cut from $\omega = -i0$ to $\omega = -i\infty$ produced by continuously many poles at $\omega = -ik^2 Dv_0 / \langle v_0 \rangle$ with infinitesimal residues. This situation is different from usual many-body transport phenomena^{4,5}) where for long wavelengths a discrete set of long-living diffusive (or propagating) excitations, represented by poles in the lower complex half-plane near the real axis, are separated from a continuum of strongly damped modes. However, for frequencies along the real axis the effect of the cut in the lower half-plane can here be well simulated in an N mode truncation by a finite sequence of poles at $\omega_s = -ik^2 D y_s$ with finite residues $Z_{nm}^{(N)}(y_s)$.

The finite-mode approximation improves with increasing dimension, since the coupling between the various modes, i.e. the off diagonal elements of the diffusivity matrix, decreases with increasing d and the range of eigenvalues $y_{\max} - y_{\min}$ decreases with increasing d (cf. fig. 1). In the limit $d \rightarrow \infty$ the diffusivity matrix (2.12) becomes a unit matrix. In this limit only the number density fluctuations survive as a fluctuating dynamical mode, the speed $y = v_0 / \langle v_0 \rangle$ being sharply peaked at $y = 1$.

3. **Velocity averaging**

In this section we will evaluate the fluctuation spectra $S_{nm}(k, \omega)$ of the conserved densities (2.1) by performing the canonical ensemble average (2.3) in two steps.

3.1. *Alternative way to evaluate density fluctuation spectra*

We first evaluate the microcanonical ensemble average $\langle \dots \rangle_m$ over positions $\mathbf{r}_0, \{\mathbf{r}_i\}$ and velocity directions \mathbf{v}_0 / v_0 for a fixed v_0

$$S(k, \omega; v_0) = \int_{-\infty}^{\infty} dt e^{i\omega t} \langle e^{-ik \cdot (r_0(t) - r_0)} \rangle_m, \tag{3.1}$$

and then we average over v_0

$$S_{nm}(k, \omega) = \langle S(k, \omega; v_0) f_n(H_0) f_m(H_0) \rangle. \tag{3.2}$$

It is the above number density fluctuation spectrum $S(k, \omega; v_0)$ evaluated in a microcanonical ensemble of hard sphere Lorentz systems which has mostly been studied so far in the literature. It can be expressed in terms of a complex generalized diffusivity $D(k, \omega; v_0)$ which for long wavelengths can well be approximated by its $k = 0$ limit

$$D(k = 0, \omega; v_0) = D \frac{v_0}{\langle v_0 \rangle} \frac{\psi(\omega/v)}{\psi(0)}. \tag{3.3}$$

Here $\psi(\omega/v) = \psi((\omega/\langle v \rangle)(\langle v_0 \rangle/v_0))$ is the Laplace transform of the velocity autocorrelation function (2.10) and $v/\langle v \rangle = v_0/\langle v_0 \rangle$. Hence for small k

$$S_{nm}(k, \omega) = -\text{Im} \left\langle \frac{f_n(H_0) f_m(H_0)}{\omega + ik^2 D \frac{v_0}{\langle v_0 \rangle} \left(\psi \left(\frac{\omega}{\langle v \rangle} \frac{\langle v_0 \rangle}{v_0} \right) \right) / \psi(0)} \right\rangle. \tag{3.4}$$

Obviously the previously derived infinite mode result $S_{nm}^{(\infty)}(k, \omega)$ (2.16) is obtained from (3.4) by taking the proper ‘‘hydrodynamic’’ limit $\omega \rightarrow 0$ in the generalized diffusivity (3.3).

3.2. Frequency-dependent diffusivity $D(\omega; v_0)$

We will now investigate the effect of the frequency dependence in $D(k = 0, \omega; v_0)$ (3.3) upon the low-frequency behaviour of $S_{nm}(k, \omega)$. Since even for $\omega \ll \langle v \rangle$ there are contributions to $\psi(z)$ with large arguments arising from small values of the speed v_0 in eq. (3.4), it might be expected that the ‘‘hydrodynamic’’ spectra $S_{nm}^{(\infty)}(k, \omega)$ should be altered by such contributions. However, this turns out to be true only to a very small degree since the weight of the velocity average (3.4) is dominated by contributions in the neighborhood of the average speed, $v_0 \approx \langle v_0 \rangle$.

To be more quantitative consider first the Laplace transform

$$\frac{\psi(\omega/v)}{\psi(0)} = \frac{i\nu\alpha}{\omega + i\nu\alpha} \tag{3.5}$$

of a velocity autocorrelation which decays exponentially at a rate α times the collision frequency ν (2.11) with α taken from computer experiments^{1d,6)} to be of the order of 1. The form of the memory function in (3.5) is a result from

the Boltzmann equation describing uncorrelated collisions and thus, it is adequate for low scatterer densities. Inserting (3.5) into (3.4) we obtain, e.g., in $d = 3$

$$k^2 DS_{11}(k, \omega) = a \left[1 - \frac{t_+ x_+ e^{x_+} E_1(x_+) - t_- x_- e^{x_-} E_1(x_-)}{t_+ - t_-} \right], \tag{3.6}$$

where $x_{\pm} = a(\omega/k^2 D)^2 t_{\pm}$. The dependence of

$$t_{\pm} = \frac{1}{2}(1 - 2\epsilon_k) \pm \frac{1}{2}\sqrt{1 - 4\epsilon_k}, \tag{3.7}$$

on $\epsilon_k = k^2 D/\alpha\langle v \rangle$ signals the presence of the second frequency scale $\alpha\langle v \rangle$ in addition to the diffusive one, $k^2 D$. However, in the ‘‘hydrodynamic’’ range ω , $k^2 D \ll \langle v \rangle$ the fluctuation spectra $S_{nm}(k, \omega)$ depend only weakly on the ‘‘microscopic’’ time $\langle v \rangle^{-1}$ within which the particle’s velocity loses memory of its initial direction; Even for a ratio as large as $\epsilon_k = 0.1$ the above spectrum (3.6) (dashed line in fig. 4) is very close to the pure ‘‘hydrodynamic’’ spectrum $S_{11}^{(\infty)}(k, \omega)$ (full line in fig. 4). Decreasing ϵ_k further suppresses the effect of the frequency dependence.

For larger scatterer densities the collisions become correlated and a back-scattering of the particle is observed in computer experiments⁶). This endows the memory function (3.3) with a non-Lorentzian frequency dependence. In order to investigate its influence we evaluated $S_{11}(k, \omega)$ with a velocity autocorrelation spectrum of Götze et al.²) which reproduces quite well the experimental velocity-autocorrelation function. To that end we first determined the Hilbert transform of the imaginary part $\psi''(\omega/\nu)$ of $\psi(\omega/\nu)$ and then

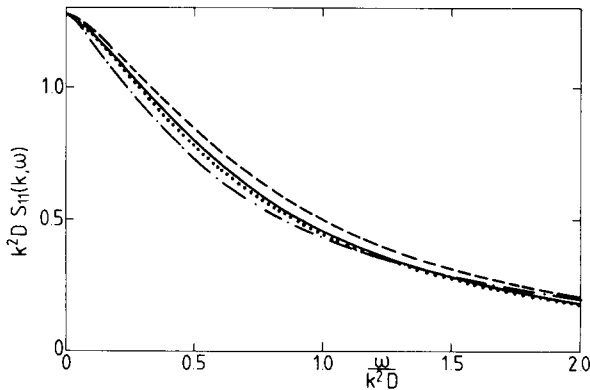


Fig. 4. Effect of a frequency-dependent generalized diffusivity $D(\omega; \nu_0)$, (3.3), upon the spectrum $k^2 DS_{11}(k, \omega)$, (3.4), of number density fluctuations. The full line represents the ‘‘hydrodynamic’’ result $k^2 DS_{11}^{(\infty)}(k, \omega)$ obtained by replacing $D(\omega; \nu_0)$ by its zero frequency value. Dots, chain curve, and dashed line denote spectra resulting from various $D(\omega; \nu_0)$ as explained in the text.

performed the average over the speeds numerically. Fig. 4 shows the resulting spectrum (dots: $k^2 D/\langle v \rangle = 0.01$; dash-dotted line: $k^2 D/\langle v \rangle = 0.1$) of number density fluctuations in $d = 3$ dimensions for a scatterer density of $n \cdot \sigma^3 = 0.4$. (The self-diffusion constant vanishes at about $n \cdot \sigma^3 \approx 0.9$.) Since the velocity spectrum $\psi''(\omega/v)/\psi''(0)$ of the Lorentzian (3.5) is for $\omega > 0$ smaller than that of Götze et al.²⁾, the density spectrum $S_{11}(k, \omega)$, (3.4), obtained by using (3.5) in the velocity average (dashed line) is larger than the corresponding density spectrum obtained by using $\psi(\omega/v)$ from Götze et al. (dash-dotted line).

The difference between the number density fluctuation spectra obtained with memory in $D(\omega; v_0)$ and without, $D(0; v_0)$, is approximately 7% at $\omega = 0.5 k^2 D$ for the value of $\epsilon_k = 0.1$ corresponding to only 10 collisions within the characteristic diffusion time $(k^2 D)^{-1}$. For smaller values of $k^2 D/\langle v \rangle$ the difference rapidly decreases: Already for $\epsilon_k = 0.01$ the two spectra are nearly indistinguishable.

4. Summary

In this work we have evaluated the low-frequency, long-wavelength fluctuation spectra of the conserved densities of a hard sphere Lorentz gas. Whereas a microcanonical ensemble of Lorentz systems has only one dynamical relevant conserved density, fluctuations of the particle's energy H_0 in a canonical ensemble imply the existence of an infinite set of conserved densities $a_n(\mathbf{k}, t) = f_n(H_0) e^{i\mathbf{k} \cdot \mathbf{r}_0(t)}$. All these slow modes are coupled among one another and their fluctuation spectra $S_{nm}^{(z)}(k, \omega)$ are determined by a superposition of infinitely many Lorentzians of different widths and infinitesimal weights, i.e. by a branch cut along the negative imaginary frequency axis.

We compared the above spectra with those obtained from a truncated set of N explicitly considered densities leading to N diffusive poles. The N -pole approximation of the spectra rapidly converges towards $S_{nm}^{(z)}(k, \omega)$. Already the two mode set of densities of particle number and energy describes reasonably well the fluctuation spectra of these two modes.

The simplicity of the hard-sphere system allowed an evaluation of the number density fluctuation spectrum $S(k, \omega; v_0)$ in a microcanonical ensemble for a particular energy (speed v_0) and subsequently obtain $S_{nm}(k, \omega) = \langle f_n(H_0) f_m(H_0) S(\mathbf{k}, \omega; v_0) \rangle$. Performing the "hydrodynamic" limit $k \rightarrow 0, \omega \rightarrow 0$ one obtains the above discussed fluctuation spectra $S_{nm}^{(z)}(k, \omega)$. The diffusivity $D(\omega; v_0)$ determining $S(k, \omega; v_0)$ in the long-wavelength limit depends on frequency and speed via an argument of the form ω/v_0 . Thus large arguments of $D(\omega; v_0)$ enter in the velocity average even if ω is small compared to the

average collision frequency $\langle\nu\rangle$. However, this frequency dependence of $D(\omega; \nu_0)$ modifies the “hydrodynamic” result $S_{nm}^{(\infty)}(k, \omega)$ for $\omega, k^2 D \ll \langle\nu\rangle$ only by a few percent even for frequencies as large as $0.1\langle\nu\rangle$. Hence the long-wavelength, low-frequency fluctuation dynamics of a canonical ensemble of hard-sphere Lorentz gases is adequately described by $S_{nm}^{(\infty)}(k, \omega)$ which in turn can well be approximated by considering only a few of the infinitely many conserved densities of this system in a standard finite mode analysis.

References

- 1) a. E.H. Hauge in Lecture Notes in Physics 31, G. Kirczenow and J. Marro, eds. (Springer, Berlin, 1974). (Sitges International School of Statistical Mechanics 1974).
 b. B.J. Alder and W.E. Alley, J. Stat. Phys. **19** (1978) 341.
 c. T. Keyes and J. Mercer, Physica **95A** (1979) 473.
 d. J.C. Lewis and J.A. Tjon, Phys. Lett. **66A** (1978) 349.
 e. W.E. Alley and B.J. Alder, Phys. Rev. Lett. **43** (1979) 653.
 f. M. Lücke, J. Phys. **C14** (1981) L113.
 g. M. Lücke, Phys. Rev. **B24** (Oct. 1981).
- 2) a. W. Götze, E. Leutheusser and S. Yip, Phys. Rev. **A23** (1981) 2634.
 b. W. Götze, E. Leutheusser and S. Yip, Phys. Rev. **A24** (1981) 1008.
- 3) M. Abramowitz and I.A. Stegun, Handbook of Mathematical Functions (Dover, New York, 1970).
- 4) See for instance: D. Forster, Hydrodynamic Fluctuations, Broken Symmetries and Correlation Functions (W.A. Benjamin, Reading, 1975).
- 5) J.J. Duderstadt and W.R. Martin, Transport Theory, (John Wiley, New York, 1979).
- 6) C. Bruin, Phys. Rev. Lett. **29** (1972) 1670; Physica **72A** (1974) 261; “A Computer Experiment on Diffusion in the Lorentz Gas”, Dissertation, (Delft Univ. Press, Delft, 1978).